Induced-dipole-electric-field contribution of atomic chains and atomic planes to the refractive index and birefringence of nanoscale crystalline dielectrics

Thomas K. Gaylord* and Yin-Jung Chang

School of Electrical and Computer Engineering and Microelectronics Research Center, Georgia Institute of Technology, Atlanta, Georgia 30332, USA

*Corresponding author: tgaylord@ece.gatech.edu

Received 16 March 2007; revised 4 May 2007; accepted 11 May 2007;
posted 21 June 2007 (Doc. ID 81103); published 31 August 2007

The induced-dipole-electric-field contribution to the refractive index at any location within a nanometer-scale dielectric is quantified by summing the electronic dipole contributions due to all the surrounding atoms in the dielectric. Using a tetragonal lattice and varying the ratio of lattice constants illustrates the important limiting chainlike and planelike behaviors. Strong polarizing effects and thus high refractive indices occur for an electric field applied along the length of a chain of atoms or applied in a planar direction to a plane of atoms. In contrast, a strong depolarizing effect and thus low refractive indices occur for an electric field applied normal to a chain of atoms or applied normal to a plane of atoms. Birefringence is increased or decreased by the simultaneous presence or absence of polarizing and depolarizing effects.

OCIS codes: 160.4760, 160.1190, 160.3130.

1. Introduction

Consistent with Moore's law, microelectronic devices, interconnects, and circuits have steadily decreased in size over the last several decades [1]. In a similar fashion, research and development are now driving modern optoelectronic devices, waveguides, and photonic integrated circuits to smaller and smaller dimensions. To be able to predict the performance accurately at nanometer-scale sizes in these structures, it is essential to know the optical properties of the constituent materials. In nanophotonic applications, dielectric materials play a central role. For particular device configurations, it may be necessary to have alternatively high index materials, low index materials, high birefringence materials, or low birefringence materials. For reliable and reproducible photonic structures, the index of refraction and the birefringence of these dielectrics must be controllable by design.

Crystalline dielectrics exhibit birefringence if the crystal system of the dielectric is noncubic [2]. Correspondingly, there are two (uniaxial) or three (biaxial) principal indices of refraction. The magnitude of the birefringence varies widely among dielectric materials [3]. The macroscopic dipole moment per unit volume, **P** (the "electric polarization"), depends on the direction of the electric field within the light wave. The inherent anisotropic nature of birefringence can be easily rationalized based on the short-range interaction of atomic electrons. In the presence of the applied electric (electromagnetic) field, the atomic electrons interact with nearby neighboring atoms largely through their atomic bonding. This is a short-range interaction and it is usually well described by considering only the nearby neighbor atoms. It can be simply represented by a spring model where the electron is effectively connected by fictitious springs with differing stiffnesses in the various directions [4]. As a result of the differing stiffnesses, the displacement of the electron depends on the direction of the applied electric field as well as its magnitude. Thus the dielectric material is anisotropic in its optical properties.

0003-6935/07/256476-07$15.00/0

However, in addition, and perhaps more importantly, in the presence of the applied electric field, atoms interact with other atoms in the dielectric through their electric-field-induced dipole moments [5]. This is a long-range interaction. This interaction acts over macroscopic distances. This interaction may cause an increase in **P** (a "polarizing" effect) or may cause a decrease in **P** (a "depolarizing" effect). A net polarizing effect increases the refractive index and relative permittivity (dielectric constant) while a net depolarizing effect decreases these quantities. In crystalline dielectrics, both polarizing and depolarizing effects may occur in the same material depending on the orientation of the applied electric field. This gives rise to birefringence. The magnitude of the polarizing and depolarizing effects is strongly dependent on the atomic structure and the amount of electric-field-induced dipole interaction that the atomic crystalline structure enables.

In this paper, the induced-dipole-electric-field contribution to the refractive index at any location within a nanometer-scale dielectric is quantified by summing the electronic dipole contributions due to all of the surrounding atoms in the dielectric. The strong polarizing effects (for a high refractive index) that occur for an electric field applied along the length of a chain of atoms or applied in a planar direction to a plane of atoms are quantified for finite nanoscale crystals. Similarly, the strong depolarizing effects (for a low refractive index) that occur for an electric field applied normal to a chain of atoms or applied normal to a plane of atoms are quantified. This is accomplished by determining the induced-dipole-electric fields in a tetragonal crystal lattice as a function of the ratio of lattice constants, c/a. In the limit as the ratio of lattice constants becomes very small or very large, this corresponds to noninteracting chains of atoms or noninteracting planes of atoms, respectively. Rather than using a limited number of dipoles in a spherical cavity (the traditional approach first introduced by Lorentz [5]), all of the surrounding dipoles are explicitly included.

2. Induced-Dipole-Electric-Field Contribution to Refractive Index

The index of refraction and the relative permittivity of a dielectric material are a measure of the electric dipole moment that is induced in the solid by an external applied electric field. The electric polarization of a dielectric is the macroscopic electric dipole moment per unit volume **P** in the material and is given by

$$\mathbf{P} = \sum_j N_j \mathbf{p}_j = \sum_j N_j \alpha_j \mathbf{E}_{local,j}, \tag{1}$$

where N_j is the concentration of atoms (number of atoms per unit volume) at the site of the jth atom, $\mathbf{p}_j$ is the electric dipole moment induced in the jth atom, α_j is the polarizability of the jth atom, and $\mathbf{E}_{local,j}$ is the local electric field at the jth atom. The local electric field is

$$\mathbf{E}_{local,j} = \mathbf{E}_{appl} + \mathbf{E}_{ind,j}, \tag{2}$$

where $\mathbf{E}_{appl}$ is the external applied electric field and $\mathbf{E}_{ind,j}$ is the induced electric field at the jth atom location due to all of the neighboring electric dipoles. The local field is also called the polarizing field since it is producing the electric polarization. The induced electric field, $\mathbf{E}_{ind,j}$, is most frequently represented as [5–7]:

$$\mathbf{E}_{ind,j} = \mathbf{E}_{depol} + \mathbf{E}_2 + \mathbf{E}_3, \tag{3}$$

where $\mathbf{E}_{depol}$ is the depolarizing field due to the polarization charges on the outer surface of the dielectric. The effective surface charge density on this outer surface is $\hat{n} \cdot \mathbf{P}$ where $\hat{n}$ is the unit vector directed normally outward from the surface. The field $\mathbf{E}_{depol}$ depends on the shape of the sample [6,7]. According to the procedure first introduced by Lorentz [5], $\mathbf{E}_2$ is the field due to polarization charges on the surface of a fictitious spherical cavity centered on the reference atom. In the literature, $\mathbf{E}_2$ is also referred to as the Lorentz field. The quantity $\mathbf{E}_3$ is the field at the reference atom location due to other dipoles lying within the sphere. The radius of the sphere is chosen to be sufficiently large such that the dielectric beyond the spherical cavity behaves as an infinite continuous homogeneous medium having the average macroscopic properties of the dielectric. However, in the present treatment, $\mathbf{E}_{ind,j}$ is evaluated directly. It is not divided as in the traditional Lorentz approach. The electric susceptibility may be defined as

$$\chi = \frac{P}{\epsilon_0 E_{macro}}, \tag{4}$$

where E_{macro} is the magnitude of the macroscopic field, which is $\mathbf{E}_{macro} = \mathbf{E}_{appl} + \mathbf{E}_{depol}$ or otherwise, $\mathbf{E}_{macro} = \mathbf{E}_{appl} - N\mathbf{P}/\epsilon_0$ where N is the depolarization factor, which can vary from zero (a field in the plane of a thin slab or along the axis of a long circular cylinder) to unity (with the field normal to a thin slab). The quantity E_{macro} is also known as the Maxwell field since it is the field that is appropriate for Maxwell's equations. Using this result, the susceptibility is

$$\chi = \frac{1}{\epsilon_0 E_{appl}/P - N}. \tag{5}$$

The index of refraction n and the relative permittivity (dielectric constant) ε are given by $n^2 = \varepsilon = 1 + \chi$

and so

$$n^2 = \varepsilon = 1 + \frac{1}{\epsilon_0 \Big/ \Big[\sum_j N_j \alpha_j (1 + E_{ind,j}/E_{appl})\Big] - N}. \quad (6)$$

For the practical case of a thin slab with the field normal to the slab (such as a deposited thin film with electrical contacts of the planar surfaces), then $N = 1$ and

$$n^2 = \varepsilon = \frac{1}{1 - \Big[\sum_j N_j \alpha_j (1 + E_{ind,j}/E_{appl})\Big] \Big/ \epsilon_0}. \quad (7)$$

In either case [Eq. (6) or (7)], the refractive index and the relative permittivity increase with the increasing strength of the induced electric field $E_{ind,j}$ and decrease with the decreasing induced electric field.

3. Induced-Dipole-Electric Field in Crystal Lattices

In infinite cubic crystal lattices, the induced-dipole electric field is identically zero due to the crystalline symmetry. However, in noncubic crystals the induced field is nonzero. In these crystal lattices, the induced field may be parallel to the applied electric field, a "polarizing" effect that increases the index or it may be antiparallel to the applied field producing a "depolarizing" effect that decreases the index. To quantify the magnitude of these effects, a tetragonal lattice is treated as a representative case.

Given a finite tetragonal lattice ($a = b \neq c$, $\alpha = \beta = \gamma = 90°$) array of identical atoms, and an applied electric field in the x direction (along a) and in the z direction (along c), what is the induced-dipole contribution to the electric field at the location of an arbitrarily selected atom? How does this induced-dipole field vary with a and c? These questions are addressed by considering an atomic array with $(M_x^- + M_x^+ + 1) \times (M_y^- + M_y^+ + 1) \times (M_z^- + M_z^+ + 1)$ atoms in the $\pm x$, $\pm y$, and $\pm z$ directions, respectively. The atom where the field is to be calculated is located at $x = y = z = 0$. Each x, y (horizontal) plane has $(M_x^- + M_x^+ + 1) \times (M_y^- + M_y^+ + 1)$ atoms. There are M_z^+ horizontal planes above the $z = 0$ layer and M_z^- horizontal layers below the $z = 0$ layer. The applied electric field induces a dipole moment $\mathbf{p}$ in each atom. The direction of the dipole is the same as that of the applied field. Each dipole produces its own field given by

$$\mathbf{E} = \frac{3(\mathbf{p} \cdot \mathbf{r})\mathbf{r} - r^2 \mathbf{p}}{4\pi\epsilon_0 r^5}, \quad (8)$$

where $\mathbf{r}$ is the vector from the dipole to the point where the field is being obtained and ϵ_0 is the permittivity of free space. For an applied field and thus a dipole in the z direction, the resulting induced field $\mathbf{E}^z$ is

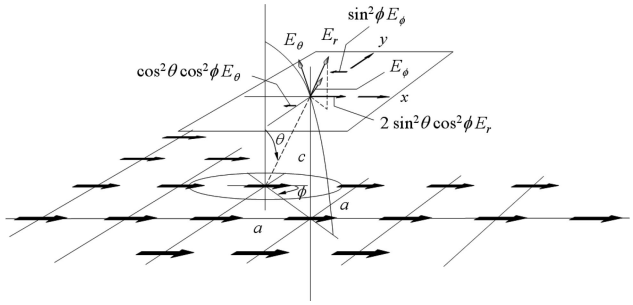

Fig. 1. Single plane of dipoles oriented in the x direction and the components of the electric field due to one of the dipoles.

$$\mathbf{E}^z = \frac{p}{4\pi\epsilon_0 r^3}\big(2\cos\theta\hat{r} + \sin\theta\hat{\theta}\big), \quad (9)$$

where θ is the angle from the axis of the dipole to the point where the field is being obtained and ^ represents the unit vector. The configuration for a field applied in the x direction is shown in Fig. 1. The total induced field $\mathbf{E}_{ind}$ is the vector sum of all the individual induced-dipole-electric fields at the particular atom where the field is being determined. For an applied field and thus a dipole in the x direction, the resulting field $\mathbf{E}^x$ is given in Appendix A. The primary component is in the x direction. This field $\mathbf{E}_x{}^x$ is given by Eq. (A1). The secondary components are in the y and z directions and are given by $\mathbf{E}_y{}^x$ and $\mathbf{E}_z{}^x$ and are also provided in Appendix A. As described by these expressions, in general, the induced-dipole-electric field is not in the same direction as the applied field. There is a fringing field that becomes more noticeable near the edges and corners of the dielectric volume. For these rectangular solids, along the axis of symmetry parallel to the applied field, the induced electric field is in the same direction as the applied field. For an applied field in the z direction, the total induced field at the reference atom location is given in Appendix B. The primary component of this field is $\mathbf{E}_z{}^z$. The secondary components are $\mathbf{E}_x{}^z$ and $\mathbf{E}_y{}^z$.

Linear chains of atoms of varying lengths can be analyzed with these expressions. A chain with a single-atom cross section corresponds to $M_x^- = M_x^+ = M_y^- = M_y^+ = 0$. A chain with a 3×3 nine-atom cross section corresponds to $M_x^- = M_x^+ = M_y^- = M_y^+ = 1$. A chain with a 5×5 25-atom cross section corresponds to $M_x^- = M_x^+ = M_y^- = M_y^+ = 2$ and so forth. Example results for the normalized induced electric fields E_{ind} at the center atom of the chain for these cases are shown in Fig. 2 for a single-atom cross-section chain, a nine-atom cross-section chain, and a 25-atom cross-section chain. For these symmetric cases the induced electric field is in the same

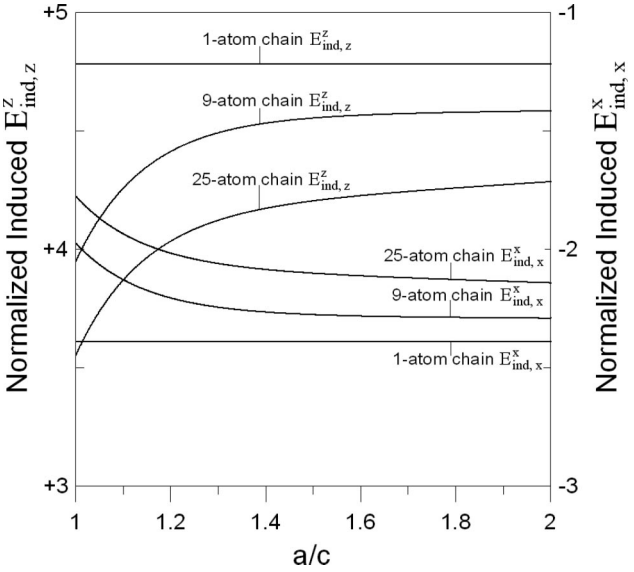

Fig. 2. x component of the normalized-induced-dipole-electric field for an applied field in the x direction, $E_{ind,x}{}^{x}$, and the z component of the normalized-induced-dipole electric field for an applied field in the z direction, $E_{ind,z}{}^{z}$, versus a/c at the reference atom at the center of the chain for single-atom-cross-section chains, nine-atom-cross-section chains, and for 25-atom-cross-section chains. All chains are 17 atoms in length. A field along the chain is highly polarizing and a field normal to the chain is highly depolarizing. Both effects are enhanced for larger values of a/c (greater separation between chains of atoms).

direction as the applied field. There are eight atoms above ($M_z{}^{+} = 8$) and eight atoms below ($M_z{}^{-} = 8$) the $x = y = z = 0$ reference atom making the chains 17 atoms in length. For a field applied in the $+x$ direction (normal to the chain), the normalized induced-dipole electric field is strongly in the $-x$ direction (depolarizing) from -1.78 to -2.39 for $1 \leq a/c \leq 2$. For an applied field in the $+z$ direction (along the chain of atoms), the normalized induced-dipole field is strongly in the $+z$ direction (polarizing) from $+3.55$ to $+4.58$ for $1 \leq a/c \leq 2$. As the distance between individual chains increases (a/c increases), the more noninteracting the chains become. In this situation the chains act like isolated chains, and the polarizing effect becomes more like that of a single chain. In the limit of a/c approaches ∞, the chains of atoms are completely noninteracting. For a single chain of atoms that is infinite in length, the maximum polarizing (applied field parallel to the chain) and the maximum depolarizing (applied field normal to the chain) effects are obtained. The resulting normalized induced fields are given in Table 1.

Planes of atoms of arbitrary size can likewise be analyzed. A single plane corresponds to $M_z{}^{-} = M_z{}^{+} = 0$. One plane above and one plane below the $z = 0$ reference plane corresponds to $M_z{}^{+} = M_z{}^{-} = 1$. Two planes above and two planes below the reference plane correspond to $M_z{}^{+} = M_z{}^{-} = 2$ and so forth. Example results for the normalized induced electric fields E_{ind} at the $z = 0$ plane at the $x = y = 0$ atom for these cases are shown in Fig. 3 for a 9×9 81-atom single-plane case, a three-plane case, and a five-plane case. For these symmetric cases the induced electric field is again in the same direction as the applied field. For a field applied in the $+x$ direction (parallel to the planes of atoms), the normalized induced-dipole electric field is strongly in the $+x$ direction (polarizing) from $+1.38$ to $+3.89$ for $1 \leq c/a \leq 2$. For an applied field in the $+z$ direction (normal to the planes of atoms), the normalized induced-dipole field is strongly in the $-z$ direction (depolarizing) from -2.77 to -7.78 for $1 \leq c/a \leq 2$. As the distance between individual planes increases (c/a increases), the more noninteracting the planes become. In this situation the planes act like isolated planes and the polarizing effect becomes like that of

Table 1. Normalized-Induced-Dipole-Electric Field in the Limit of an Infinitely Long Chain and an Infinitely Wide Plane of Dipoles

	Normalized-Induced-Electric Field	
	$E_{ind,z}{}^{z} \Big/ \left(\frac{p}{4\pi\epsilon_0 c^3}\right)$	$E_{ind,x}{}^{x} \Big/ \left(\frac{p}{4\pi\epsilon_0 a^3}\right)$
	$E_{ind,x}{}^{x} \Big/ \left(\frac{p}{4\pi\epsilon_0 c^3}\right)$	$E_{ind,z}{}^{z} \Big/ \left(\frac{p}{4\pi\epsilon_0 a^3}\right)$
	Linear Lattice Chain	Square Lattice Plane
Polarizing	$+4.8082$ ($E \parallel$ chain)	$+4.5113$ ($E \parallel$ plane)
Depolarizing	-2.4041 ($E \perp$ chain)	-9.0226 ($E \perp$ plane)

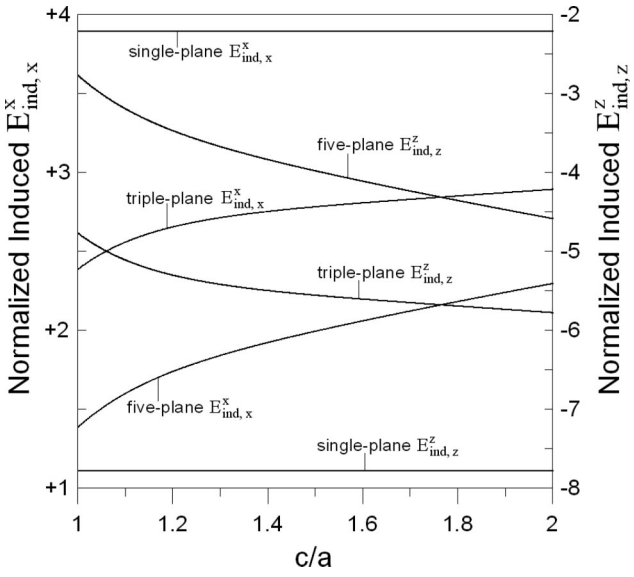

Fig. 3. x component of the normalized-induced-dipole electric field for an applied field in the x direction, $E_{ind,x}{}^{x}$, and the z component of the normalized-induced-dipole electric field for an applied field in the z direction, $E_{ind,z}{}^{z}$, versus c/a at the reference atom at the center of a single 81-atom plane, for a triple 81-atom plane, and for five 81-atom planes. A field in the plane of atoms is highly polarizing and a field normal to the plane is highly depolarizing. Both effects are enhanced for larger values of c/a (greater separation between planes of atoms).

a single plane. In the limit of c/a approaches ∞, the planes of atoms are completely noninteracting. For a single plane of atoms that is infinite in the lateral extent, the maximum polarizing (applied field parallel to the plane) and the maximum depolarizing (applied field normal to the plane) effects are obtained. For the field parallel to the plane, all directions such as the x direction, the y direction, the $x = y$ direction, etc. produce the same magnitude of polarizing effect. The resulting normalized induced fields are given in Table 1. Overall, the strongest polarizing effect (+4.81) occurs for a field applied along the length of a chain of atoms and the strongest depolarizing effect (−9.02) occurs for a field applied normal to a plane of atoms. For an infinite chain of atoms, the maximum polarizing induced field is twice the magnitude of the maximum depolarizing induced field for the same chain. Correspondingly, for an infinite plane of atoms, the maximum depolarizing induced field is twice the magnitude of the maximum polarizing induced field for the same plane.

For an electromagnetic wave propagating in such a dielectric, the electric field of the wave acts as the applied field E_{appl}. From Eq. (6), the refractive indices at the site of the jth atom are thus

$$n^x = n^x\left(E_{ind,j}{}^x\right), \qquad n^y = n^y\left(E_{ind,j}{}^y\right), \qquad n^z = n^z\left(E_{ind,j}{}^z\right), \tag{10}$$

for the electric field along the x, y, and z directions, respectively. For a configuration of atoms that is symmetric in the x and y directions about the center reference atom, then $n^x = n^y$ and the behavior is that of a uniaxial birefringent material with a birefringence of

$$(\Delta n)_{biref} = n^z - n^x. \tag{11}$$

If $(\Delta n)_{biref} > 0$, then it is positive uniaxial birefringence (such as quartz). If $(\Delta n)_{biref} < 0$, then it is negative uniaxial birefringence (such as calcite).

4. Summary and Discussion

The induced-dipole electric field in nanometer-scale dielectrics has been quantified by summing the electronic contributions due to all of the individual atoms in the dielectric volume. A tetragonal lattice has been used as the representative crystal lattice. The ratio of lattice constants has been varied to illustrate chainlike or planelike behaviors. In the limit as the ratio of lattice constants becomes very small or very large, this corresponds to noninteracting chains of atoms or noninteracting planes of atoms. Strong polarizing effects and thus high refractive indices are shown to occur for an electric field applied along the length of a chain of atoms or applied in a planar direction to a plane of atoms. Similarly, a strong depolarizing effect and thus low refractive indices are shown to occur for an electric field applied normal to a chain of atoms or applied normal to a plane of atoms.

The present results are clearly consistent with well-known concepts of needlelike or chainlike structures (e.g., many liquid crystals) being positive birefringent materials. The electromagnetic wave with its electric field along the needle (chain) experiences a larger refractive than for the field normal to the needles. Quartz, which can be simply modeled as helices of oxygen atoms, is also positive birefringent. The wave with its electric field along the helix axis experiences a higher refractive index. Obviously, a helix is rather like a chain. Similarly, materials that can be modeled as planes of oxygen atoms (e.g., lithium niobate) are negative birefringent materials. The wave with its electric field in the plane of the atoms experiences a larger refractive index. Materials with zig-zag plane structures would be expected to exhibit similar characteristics.

Using the present approach, the induced-dipole electric field can be calculated at any location in the dielectric volume including at the edges and the corners. Appropriately accounting for the medium surrounding the dielectric, the variation of the induced field can be mapped throughout the dielectric volume. The present approach enables a systematic strategy that can be used to develop, identify, and evaluate nanoscale high-refractive-index dielectrics and low-refractive-index dielectrics at visible frequencies. At low frequencies (dc through microwaves) there would generally be an ionic contribution as well. Nevertheless, the present approach can be used to evaluate the electronic contribution for the development of high-dielectric-constant materials for applications such as the gate oxide in complementary metal-oxide semiconductor (CMOS) transistors and as the dielectric material in decoupling capacitors in CMOS interconnect layers. Similarly, the present approach can be used in the development of low-dielectric-constant materials for applications such as the interlayer dielectric for use with copper interconnects in CMOS integrated circuits.

Appendix A: Induced-Dipole-Electric-Field for Applied Field in the x Direction

The x component of the induced-dipole-electric field for an applied electric field in the x direction is $\mathbf{E}_{ind,x}{}^x$ and is given by Eq. (A1). The ten terms in this equation represent the contributions due to dipoles (1) in the first quadrant, (2) in the second quadrant, (3) in the third quadrant, (4) in the fourth quadrant, (5) along the $+x$ axis, (6) along the $-x$ axis, (7) along the $+y$ axis, (8) along the $-y$ axis, (9) along the $+z$ axis, and (10) along the $-z$ axis with the origin being the observation point (the atom where the field is to be determined).

$$\mathbf{E}_{ind,x}{}^{x} = \hat{x}\,\frac{p}{4\pi\epsilon_0}\left\{\left(\sum_{k=-M_z^-}^{M_z^+}\sum_{i^+=1}^{M_x^+}\sum_{j^+=1}^{M_y^+}\frac{\psi_x{}^{x}(\theta,\ \phi)}{\left[(i^+a)^2+(j^+a)^2+(kc)^2\right]^{3/2}}\right)\right|_{\substack{\phi=\pi+\tan^{-1}(j^+/i^+),\\ \theta=\theta^-\text{ for }k<0,\\ \theta=\theta^+\text{ for }k\geq 0}}$$

$$+\left(\sum_{k=-M_z^-}^{M_z^+}\sum_{i^-=1}^{M_x^-}\sum_{j^+=1}^{M_y^+}\frac{\psi_x{}^{x}(\theta,\ \phi)}{\left[(i^-a)^2+(j^+a)^2+(kc)^2\right]^{3/2}}\right)\Bigg|_{\substack{\phi=-\tan^{-1}(j^+/i^-),\\ \theta=\theta^-\text{ for }k<0,\\ \theta=\theta^+\text{ for }k\geq 0}}$$

$$+\left(\sum_{k=-M_z^-}^{M_z^+}\sum_{i^-=1}^{M_x^-}\sum_{j^-=1}^{M_y^-}\frac{\psi_x{}^{x}(\theta,\ \phi)}{\left[(i^-a)^2+(j^-a)^2+(kc)^2\right]^{3/2}}\right)\Bigg|_{\substack{\phi=\tan^{-1}(j^-/i^-),\\ \theta=\theta^-\text{ for }k<0,\\ \theta=\theta^+\text{ for }k\geq 0}}$$

$$+\left(\sum_{k=-M_z^-}^{M_z^+}\sum_{i^+=1}^{M_x^+}\sum_{j^-=1}^{M_y^-}\frac{\psi_x{}^{x}(\theta,\ \phi)}{\left[(i^+a)^2+(j^-a)^2+(kc)^2\right]^{3/2}}\right)\Bigg|_{\substack{\phi=\pi-\tan^{-1}(j^-/i^+),\\ \theta=\theta^-\text{ for }k<0,\\ \theta=\theta^+\text{ for }k\geq 0}}$$

$$+\left(\sum_{k=-M_z^-}^{M_z^+}\sum_{i^+=1}^{M_x^+}\frac{\psi_x{}^{x}(\theta,\ \phi)}{\left[(i^+a)^2+(kc)^2\right]^{3/2}}\right)\Bigg|_{\substack{\phi=\pi,\\ \theta=\theta^-\text{ for }k<0,\\ \theta=\theta^+\text{ for }k\geq 0}}$$

$$+\left(\sum_{k=-M_z^-}^{M_z^+}\sum_{i^-=1}^{M_x^-}\frac{\psi_x{}^{x}(\theta,\ \phi)}{\left[(i^-a)^2+(kc)^2\right]^{3/2}}\right)\Bigg|_{\substack{\phi=0,\\ \theta=\theta^-\text{ for }k<0,\\ \theta=\theta^+\text{ for }k\geq 0}}$$

$$+\left(\sum_{k=-M_z^-}^{M_z^+}\sum_{j^+=1}^{M_y^+}\frac{\psi_x{}^{x}(\theta,\ \phi)}{\left[(j^+a)^2+(kc)^2\right]^{3/2}}\right)\Bigg|_{\substack{\phi=-\pi/2,\\ \theta=\theta^-\text{ for }k<0,\\ \theta=\theta^+\text{ for }k\geq 0}}$$

$$+\left(\sum_{k=-M_z^-}^{M_z^+}\sum_{j^-=1}^{M_y^-}\frac{\psi_x{}^{x}(\theta,\ \phi)}{\left[(j^-a)^2+(kc)^2\right]^{3/2}}\right)\Bigg|_{\substack{\phi=\pi/2,\\ \theta=\theta^-\text{ for }k<0,\\ \theta=\theta^+\text{ for }k\geq 0}}$$

$$+\left(\sum_{k=1}^{M_z^+}\frac{\psi_x{}^{x}(\theta,\ \phi)}{(kc)^3}\right)\Bigg|_{\substack{\phi=0,\\ \theta=\pi}}+\left(\sum_{k=-M_z^-}^{-1}\frac{\psi_x{}^{x}(\theta,\ \phi)}{(|k|c)^3}\right)\Bigg|_{\substack{\phi=0,\\ \theta=0}}\Bigg\}, \tag{A1}$$

where

$$\psi_x{}^{x}(\theta,\ \phi) = (3\sin^2\theta - 1)\cos^2\phi - \sin^2\phi, \tag{A2}$$

$$\theta^- = \tan^{-1}\left[(i^\pm)^2 + (j^\pm)^2\right]^{1/2}a/|k|c, \tag{A3}$$

$$\theta^+ = \pi/2 + \tan^{-1}|k|c/\left[(i^\pm)^2 + (j^\pm)^2\right]^{1/2}a, \tag{A4}$$

and $(i^\pm, j^\pm, k)$ represent the set of indices describing the coordinates of a dipole contributing to the field at the observation point. The y component of the induced-dipole-electric field for an applied electric field in the x direction is $\mathbf{E}_{ind,y}{}^{x}$. It is given by an expression such as that in Eq. (A1) except that the resulting field is in the y direction and $\psi_x{}^{x}$ is replaced by $\psi_y{}^{x}$, where

$$\psi_y{}^{x}(\theta,\ \phi) = 3\ \sin^2\theta\cos\phi\sin\phi. \tag{A5}$$

Similarly, the z component of the induced-dipole-electric field for an applied electric field in the x direction is $\mathbf{E}_{ind,z}{}^{x}$. It is also given by an expression such as that in Eq. (A1) except that the resulting field is in the z direction and $\psi_x{}^{x}$ is replaced by $\psi_z{}^{x}$, where

$$\psi_z{}^{x}(\theta,\ \phi) = 3\cos\theta\sin\theta\cos\phi. \tag{A6}$$

Appendix B: Induced-Dipole-Electric Field for Applied Field in the *z* Direction

The z component of the induced-dipole-electric field for an applied electric field in the z direction is $\mathbf{E}_{ind,z}{}^{z}$ and is given by Eq. (B1). Again, the ten terms represent the contributions due to dipoles (1) in the first quadrant, (2) in the second quadrant, (3) in the third quadrant, (4) in the fourth quadrant, (5) along the $+x$ axis, (6) along the $-x$ axis, (7) along the $+y$ axis, and (8) along the $-y$ axis, (9) along the $+z$ axis, and (10) along the $-z$ axis with the origin being the atom

where the field is to be determined. For the z component of the field there is no dependence on ϕ.

$$\psi_y^{\,z}(\theta,\ \phi) = 3\cos\theta\sin\theta\sin\phi. \tag{B4}$$

$$\begin{aligned}
\mathbf{E}_{ind,z}{}^{z} = \hat{z}\,\frac{p}{4\pi\epsilon_0}\Bigg\{ & \left(\sum_{k=-M_z^-}^{M_z^+}\sum_{i^+=1}^{M_x^+}\sum_{j^+=1}^{M_y^+}\frac{\psi_z^{\,z}(\theta)}{\left[(i^+a)^2+(j^+a)^2+(kc)^2\right]^{3/2}}\right)\Bigg|_{\substack{\theta=\theta^- \text{ for } k<0,\\ \theta=\theta^+ \text{ for } k\geq 0}} \\
& + \left(\sum_{k=-M_z^-}^{M_z^+}\sum_{i^-=1}^{M_x^-}\sum_{j^+=1}^{M_y^+}\frac{\psi_z^{\,z}(\theta)}{\left[(i^-a)^2+(j^+a)^2+(kc)^2\right]^{3/2}}\right)\Bigg|_{\substack{\theta=\theta^- \text{ for } k<0,\\ \theta=\theta^+ \text{ for } k\geq 0}} \\
& + \left(\sum_{k=-M_z^-}^{M_z^+}\sum_{i^-=1}^{M_x^-}\sum_{j^-=1}^{M_y^-}\frac{\psi_z^{\,z}(\theta)}{\left[(i^-a)^2+(j^-a)^2+(kc)^2\right]^{3/2}}\right)\Bigg|_{\substack{\theta=\theta^- \text{ for } k<0,\\ \theta=\theta^+ \text{ for } k\geq 0}} \\
& + \left(\sum_{k=-M_z^-}^{M_z^+}\sum_{i^+=1}^{M_x^+}\sum_{j^-=1}^{M_y^-}\frac{\psi_z^{\,z}(\theta)}{\left[(i^+a)^2+(j^-a)^2+(kc)^2\right]^{3/2}}\right)\Bigg|_{\substack{\theta=\theta^- \text{ for } k<0,\\ \theta=\theta^+ \text{ for } k\geq 0}} \\
& + \left(\sum_{k=-M_z^-}^{M_z^+}\sum_{i^+=1}^{M_x^+}\frac{\psi_z^{\,z}(\theta)}{\left[(i^+a)^2+(kc)^2\right]^{3/2}}\right)\Bigg|_{\substack{\theta=\theta^- \text{ for } k<0,\\ \theta=\theta^+ \text{ for } k\geq 0}} \\
& + \left(\sum_{k=-M_z^-}^{M_z^+}\sum_{i^-=1}^{M_x^-}\frac{\psi_z^{\,z}(\theta)}{\left[(i^-a)^2+(kc)^2\right]^{3/2}}\right)\Bigg|_{\substack{\theta=\theta^- \text{ for } k<0,\\ \theta=\theta^+ \text{ for } k\geq 0}} \\
& + \left(\sum_{k=-M_z^-}^{M_z^+}\sum_{j^+=1}^{M_y^+}\frac{\psi_z^{\,z}(\theta)}{\left[(j^+a)^2+(kc)^2\right]^{3/2}}\right)\Bigg|_{\substack{\theta=\theta^- \text{ for } k<0,\\ \theta=\theta^+ \text{ for } k\geq 0}} \\
& + \left(\sum_{k=-M_z^-}^{M_z^+}\sum_{j^-=1}^{M_y^-}\frac{\psi_z^{\,z}(\theta)}{\left[(j^-a)^2+(kc)^2\right]^{3/2}}\right)\Bigg|_{\substack{\theta=\theta^- \text{ for } k<0,\\ \theta=\theta^+ \text{ for } k\geq 0}} \\
& + \left(\sum_{k=1}^{M_z^+}\frac{\psi_z^{\,z}(\theta,\ \phi)}{(kc)^3}\right)\Bigg|_{\substack{\phi=0,\\ \theta=\pi}} + \left(\sum_{k=M_z^-}^{-1}\frac{\psi_z^{\,z}(\theta,\ \phi)}{(|k|c)^3}\right)\Bigg|_{\substack{\phi=0,\\ \theta=0}}\Bigg\},
\end{aligned} \tag{B1}$$

where

$$\psi_z^{\,z}(\theta) = 3\cos^2\theta - 1, \tag{B2}$$

and θ^- and θ^+ are given by Eqs. (A3) and (A4). When $\theta = \cos^{-1}(1/\sqrt{3}) = 54.736°$, the z component of the dipole field is zero. The x component of the induced-dipole-electric field for an applied electric field in the z direction is $\mathbf{E}_{ind,x}{}^{z}$. It is given by an expression such as Eq. (A1) except that the resulting field is in the x direction and $\psi_x^{\,x}$ is replaced by $\psi_x^{\,z}$, where

$$\psi_x^{\,z}(\theta,\ \phi) = \psi_z^{\,x}(\theta,\ \phi) = 3\cos\theta\sin\theta\cos\phi. \tag{B3}$$

Similarly, the y component of the induced-dipole-electric field for an applied electric field in the z direction is $\mathbf{E}_{ind,y}{}^{z}$. It is also given by an expression such as Eq. (A1) except that the resulting field is in the y direction and $\psi_x^{\,x}$ is replaced by $\psi_y^{\,z}$, where

This work was performed as part of the Interconnect Focus Center research program and was supported by the Microelectronics Advanced Research Corporation (MARCO) and the Defense Advanced Research Projects Agency (DARPA).

References

1. E. Mollick, "Establishing Moore's law," Ann. Hist. Comput. **28,** 62–75 (2006).
2. J. F. Nye, *Physical Properties of Crystals* (Oxford U. Press, 1957).
3. A. Yariv and P. Yeh, *Optical Waves in Crystals* (Wiley-Interscience, 1984).
4. G. R. Fowles, *Introduction to Modern Optics* (Holt, Rinehart, and Winston, 1968).
5. H. A. Lorentz, *The Theory of Electrons* (Teubner, 1909).
6. H. Froehlich, *Theory of Dielectrics: Dielectric Constant and Dielectric Loss,* 2nd ed. (Oxford U. Press, 1958).
7. C. Kittel, *Introduction to Solid State Physics,* 5th ed. (Wiley, 1976).